Journal of Materials and Environmental Science
ISSN : 2028-2508
CODEN : JMESCN

J. Mater. Environ. Sci., 2020, Volume 11, Issue 5, Page 684-694

http://www.jmaterenvironsci.com

Discovery of novel potential anti-Alzheimer hydrazones derivatives using 3D QSAR and molecular docking studies

Khalil EL Khatabi[1], Ilham Aanouz[1], Reda EL-Mernissi[1], Ayoub Khaldan[1], Mohammed Aziz Ajana[1], Mohammed Bouachrine[1] and Tahar Lakhlifi[1]

[1]Molecular chemistry and Natural Substances Laboratory. Faculty of Science, University of Moulay Ismail, Meknes, Morocco.

Received 22 Feb 2020,
Revised 18 March 2020,
Accepted 18 March 2020

Keywords

- ✓ Computational study,
- ✓ 3D-QSAR,
- ✓ Molecular Docking,
- ✓ Hydrazones,
- ✓ Acetylcholinesterase.

a.ajanamohammed@fs.umi.ac.ma
Phone: +212672603899

Abstract

The acetylcholinesterase inhibitors play a significant role in anti-Alzheimer drug development. In this current study, a series of 20 piperidinehydrazide-hydrazones derivatives reported from a published study was selected as a novel class of highly potent acetylcholinesterase inhibitors to combat Alzheimer's disease, and was subjected to 3D-QSAR studies including CoMFA and CoMSIA. Further, the significant statistical reliability and high predictability of the CoMFA (Q^2=0.604, R^2=0.863, r_{ext}^2=0.700) and CoMSIA (Q^2=0.606, R^2=0.854, r_{ext}^2=0.647) models was validated by an external test set of 6 compounds. Moreover, the Three-dimensional contour maps obtained from selected models revealed the relationship between molecular features and inhibitory activity which gives useful insight into the development of a new generation of inhibitors against Alzheimer showing effective acetylcholinesterase inhibition. Based on the X-ray crystallized complex (PDB code: 1EVE), the molecular docking method was investigated using Surflex-dock as an approach to obtain reliable conformation for molecular alignment and confirm the 3D-QSAR result supporting the stability of the predicted molecules in the receptor.

1. Introduction

Alzheimer's disease is a degrading and irreversible neurodegenerative disorder associated with loss of brain functions. People with Alzheimer's disease lose their abilities at varying levels. It is manifested clinically into psychological symptoms that collectively form cognitive dysfunction and the failure of thinking skills through the progressive degeneration of central nervous system neurons [1, 2].

Combinatorial reasons are key pathological features in the appearance and progression of the disease such as genetic, environmental influences and lifestyle. The main causes of AD are deficits in cholinergic neurotransmission [3], bio metals dysfunction [4, 5], cellular accumulation of β-amyloid (Aβ) plaques; damaged amyloid proteins build to toxic levels, causing call damage and death [6], inflammation and increased oxidative stress [7], destabilization of calcium homeostasis [8] and accumulation of tau-protein hyper phosphorylation [9].

The position in the brain where the blood flow of a series of minor strokes or changes in the brain determines the severity of the problem and the effect which can result in death of the brain tissue. Acetylcholinesterase (AChE) and butyryl-cholinesterase (BChE) are two enzymes that are widespread in the body with huge amounts targeting neurotransmitters such as ACh and other choline esters. It was suggested that AChE played a major role in regulating, whereas BChE has no big influence on the healthy brain. Acetylcholine (ACh) is a chemical compound called neurotransmitter that is released at the end of a nerve cell after a nerve impulse arrives which is transmitted at synapses. It plays a vital therapeutic role in elevating Ach levels. Many research studies are still underway to find new antioxidant agents with improved efficacy to inhibit AChE and BuChE for the processing of Alzheimer's Disease.

In order to design more potent acetylcholinesterase inhibitors with better binding infinity, a set of biologically evaluated synthetic Alzheimer of piperidine hydrazide-hydrazones derivatives were used to build models executing the three-dimensional quantitative structure-activity relationship (3D-QSAR) and predict their antioxidant activity using Comparative Molecular Field Analysis (CoMFA) and Comparative Molecular Similarity Indices Analysis (CoMSIA) methods [10, 11]. The molecular docking study was performed using Surflex-docking method to identify essential site residues involved in the binding modes between the target protein 1EVE receptor and bioactive molecules and indicated the reliability safety of the proposed compounds.

2. Materials and methods

A database of experimentally reported 20 hydrazone derivatives were taken from a published study [12], the database was subdivided into two sets, 14 compounds were for training set and 6 compounds for test set which are chosen randomly to build QSAR models. The acetylcholinesterase inhibitory activities IC50 (µM) were converted to the corresponding pIC50 (pIC50 = log IC50), they are listed with their corresponding structures in Figure 1 and Table 1, respectively.

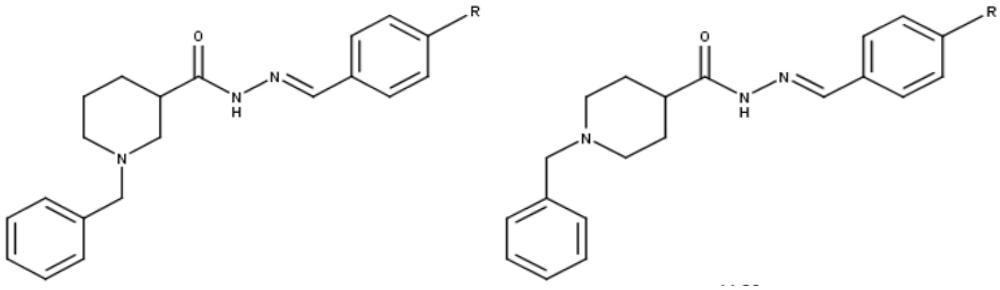

1-10 11-20

Figure 1: Chemical structures of the studied compounds.

Table 1: Chemical structures of hydrazone derivatives with (AChE) inhibitor activities.

N°	R	pIC50
1	H	5.164
2*	CH_3	4.982
3*	OCH_3	5.141
4	F	5.124
5	Cl	5.171
6	Br	5.144
7	NO_2	5.246
8	CN	5.182
9	$N(CH_3)_2$	5.181
10	$N(CH_2CH_3)_2$	5.210
11	H	5.046
12	CH_3	4.972
13	OCH_3	5.089
14	F	5.119
15*	Cl	4.992
16*	Br	5.007
17	NO_2	5.199
18*	CN	5.149
19	$N(CH_3)_2$	5.049
20*	$N(CH_2CH_3)_2$	4.945

* Test set molecules

2.1. Minimization and alignment

The 3D structures of the studied compounds were built and minimized using Sybyl program [13] under the Tripos standard force field [14], Gasteiger-Hückel atomic partial charges [15] by the Powell method with a convergence criterion of 0.01 kcal/mol Å.

The molecular alignment aims at improving 3D-QSAR models, the molecules were all aligned on the common core, N'-[(1E)-phenylmethylidene] acetohydrazide, using the simple alignment protocol in Sybyl [16]. The potent inhibitor active compound 7 was chosen as a reference. Figure 2 Shows The superimposed structures set and the common core.

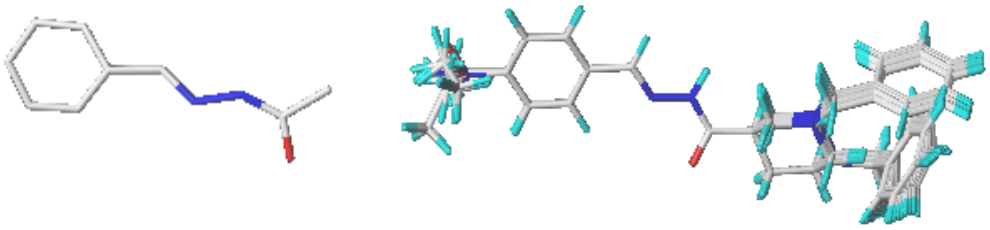

Core aligned compounds

Figure 2: 3D-QSAR aligned compounds using compound 7 as a template.

2.2. 3D QSAR results:

Based on 3D-QSAR modeling, the 3D-QSAR models were developed to analyze quantitatively, steric, electrostatic, hydrophobic, and H-bond acceptor and donor effects fields. Therefore, the contour maps of 3D-QSAR models were produced for visualizing the results and explored to explain the key structural features required for acetylcholinesterase inhibition activity.

3D-QSAR studies were carried out in standard settings with the minimum sigma (column filtering) is set to 2.0 kcal/mol, and the energy cutoff values of 30 kcal/mol [17]. Regression analysis used in this work is the cross validation PLS method [18] and the final non cross validated model is developed by an optimal number of components with the highest coefficient of cross-validated correlation Q^2 value and the lowest value of standard error predictions. Moreover, the external validation r_{ext}^2 was used using six molecules as a test set to estimate the predictive model capability of the obtained models. The best QSAR model was chosen on the basis of high Q^2, coefficient of correlation R^2 values ($Q^2 > 0.50$ and $R^2 > 0.60$) [19, 20], an optimal number of component values, and low standard error estimation (SEE). The value of r_{ext}^2 should be more than 0.6 which in turn indicates that the statistical significance generated of QSAR model is good [21].

2.3. Y-Randomization

The Y-Randomization test [22] is performed to evaluate the robustness of 3D-QSAR models. The dependent variable ($-\log IC_{50}$) is shuffled several times at random, and after each iteration, a new QSAR model is generated. The high values of the Q^2 and R2 indicate that, due to structural redundancy and chance correlation, an appropriate 3D-QSAR model cannot be produced for this dataset

2.4. Molecular Docking

To validate the contour maps results of CoMFA and CoMSIA models, the molecular docking was conducted by the Surflex-Dock [23] to explore the binding interactions between the most active compound and the new proposed compound with the highest Acetylcholinesterase inhibitor activity. The obtained results were analyzed using PyMol [24] and Discovery studio 2016 [25] softwares.

2.4.1. Macromolecule preparation

The X-ray crystal structure of TcAChE (Torpedo californica acetylcholinesterase PDB code: 1EVE, resolution: 2.5 Å) was retrieved from the RCSB data bank and its original ligand was removed then the

most active ligands from our data set and the proposed compound were docked into a protein's binding site. The protein was prepared by removing water molecules in 1EVE and the polar hydrogen atoms are added to the protein using Discovery Studio 2016.

2.4.2. Ligand preparation

The 3D structure of the representative and the proposed compounds, were geometrically optimized and energetically minimized using default parameters. These studied compounds were docked into the binding site of the acetylcholinesterase enzyme.

3. Results and discussion

Based on 3D-QSAR modeling, CoMFA and CoMSIA analyses were carried out on 14 training set compounds of 20 hydrazones derivatives which were reported as acetylcholinesterase inhibitors. Obviously, both models had satisfactory coefficient of cross-validated correlation Q^2 values of 0.604 and 0.606 and a high coefficient of determination R^2 values of 0.952 and 0.854 of training set for CoMFA and CoMSIA, respectively. The high Q^2 and R^2 values, and low SEE values with three as optimum number of components, suggest that both models possess high predictive abilities and significant statistical reliability of the QSAR models. Besides, the external predictive ability was approved using six molecules selected randomly as test set, it resulted in r_{ext}^2 values of 0.700 and 0.647 for CoMFA and CoMSIA, respectively. In CoMFA model, the proportions of steric to electrostatic contributions were found to be 57.9% and 41.1% respectively, which means that steric and electrostatic field have a great impact in the binding affinities, while in CoMSIA model, the proportions of steric, electrostatic, H-bond acceptor, H-bond donor, and hydrophobic contributions accounted for 12.4%, 35.9%, 32%, 1.7%, and 17.9%, respectively. Quantitative result in Table 2 indicated that both CoMFA and CoMSIA model were reasonable and reliable for predicting activities of inhibitors. The experimental and predicted pIC50 of training and test sets were shown in Table 3. Figure 3 shows a significant linear correlation between calculated and observed pIC50 values

Table 2: PLS Statistics of CoMFA and CoMSIA models.

Model	Q^2	R^2	SEE	F	N	r_{ext}^2	Fractions				
							Ster	Elect	Acc	Don	Hyd
CoMFA	0.604	0.952	0.031	20.94	3	0.700	0.579	0.411	-	-	-
CoMSIA	0.606	0.854	0.032	17.15	3	0.647	0.124	0.359	0.320	0.017	0.179

$R^{2:}$ Non-cross-validated correlation coefficient; Q^2: Cross-validated correlation coefficient.
r_{ext}^2: External validation correlation coefficient; SEE: Standard error of the estimate; N: Optimum number of components; F: F-test value.

The scatter plots of the experimental and predicted biological activity for the training set and test set compounds exhibited a very regular distribution of acetylcholinesterase activity values for CoMFA and CoMSIA models as shown in Fig. 3.

Table 3: Experimental and predicted activities of 20 hydrazone derivatives.

N°	pIC50	CoMFA		CoMSIA	
		predicted	Residuals	predicted	Residuals
1	5.164	5.123	0.041	5.123	0.041
2*	4.982	5.048	-0.066	5.055	-0.073
3*	5.141	5.095	0.046	5.095	0.046
4	5.124	5.156	-0.032	5.156	-0.032
5	5.171	5.147	0.024	5.147	0.024
6	5.144	5.146	-0.002	5.145	-0.001

7	5.246	5.246	0	5.245	0.001
8	5.182	5.205	-0.023	5.209	-0.027
9	5.181	5.152	0.029	5.153	0.028
10	5.210	5.204	0.006	5.205	0.005
11	5.046	5.027	0.019	5.028	0.018
12	4.972	5.025	-0.053	5.029	-0.057
13	5.089	5.079	0.010	5.078	0.009
14	5.119	5.082	0.037	5.081	0.036
15*	4.992	5.028	0.036	5.029	0.037
16*	5.007	5.027	-0.020	5.028	-0.021
17	5.199	5.183	0.016	5.181	0.014
18*	5.149	5.109	0.040	5.098	0.051
19	5.049	5.049	0	5.051	-0.002
20*	4.945	4.898	0.047	4.901	0.044

* Test set molecules.

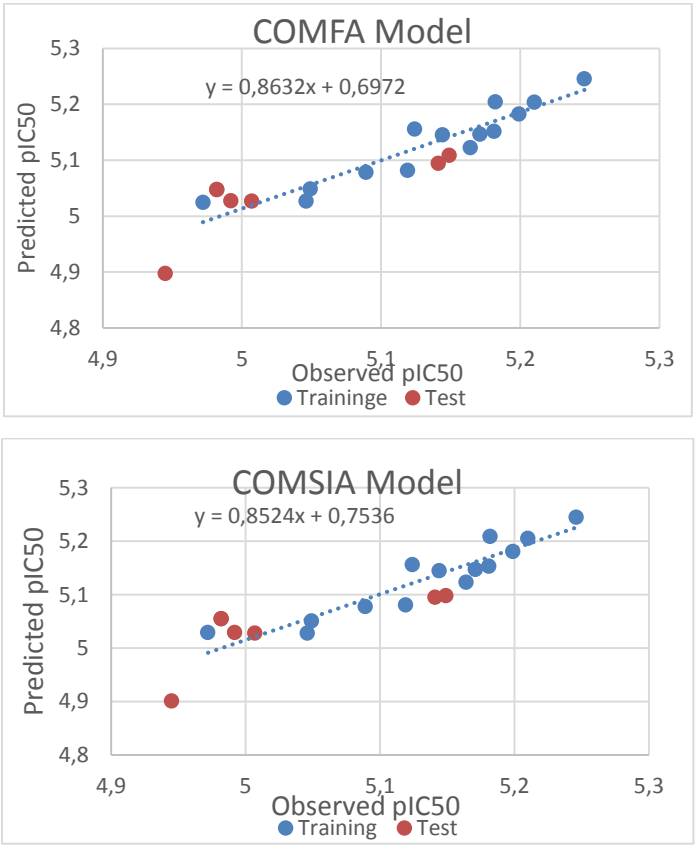

Figure 3: Graphical representation of the observed and predicted activity of training and test sets for CoMFA and CoMSIA models

3.1.Contour map analysis

The CoMFA/CoMSIA contour maps were generated to visualize the field distribution of the models where the modifications could provide an increase in the activity. The figures 4 and 5 showed the contour maps of CoMFA and CoMSIA, respectively, using compound 7 as a reference structure.

3.1.1. CoMFA contour maps

The contour maps of CoMFA electrostatic field are presented with red (20% contribution) and blue (80% contribution) colors while steric interactions are presented with green (80% contribution) and yellow (20% contribution) colored contours. In the steric field (Figure 4a), the green color indicates sterically favorable bulky substituents while the yellow color represents the opposite.

Two green contours appeared around R1 positions, indicating that bulkier groups in these regions could increase the activity, this finding might explain why the binding activity of compounds 10 (pIC50 =5.210) and compounds 7 (pIC50 =5.246), with diethylamine and nitro groups at the R1 position, are higher than compound 2 (pIC50 =4.982) consisted of methyl (–CH3) group at R1 position. The presence of yellow contour around piperidine moiety suggested that adding a bulky substitution in this region would be unfavorable for the potency. electrostatic contour map was seen with blue and red contours as shown in (Figure 4b); blue contour indicates that electropositive charge are predicted to enhance biological activity, while red contours indicate that electronegative charges are predicted to benefit activity. The small-sized red contour near R1 position indicates that the addition of electronegative substituent at this position may help increase the inhibitory activity. Besides, two blue contours are founded close to the phenyl moiety linked to piperidine and inside the phenyl indicating that substituents with electron-donating character are favored at these positions which would exhibit good anti-Alzheimer activity. These contour maps explain that compounds 7, 15, 8, 17, and 18 with electropositive character in this region may potentially function via acetylcholinesterase. Therefore, electropositive and bulkier substituents are required at the R_1 position and they can easily reach the binding pocket in the active site of the enzyme and present high acetylcholinesterase inhibition affinity.

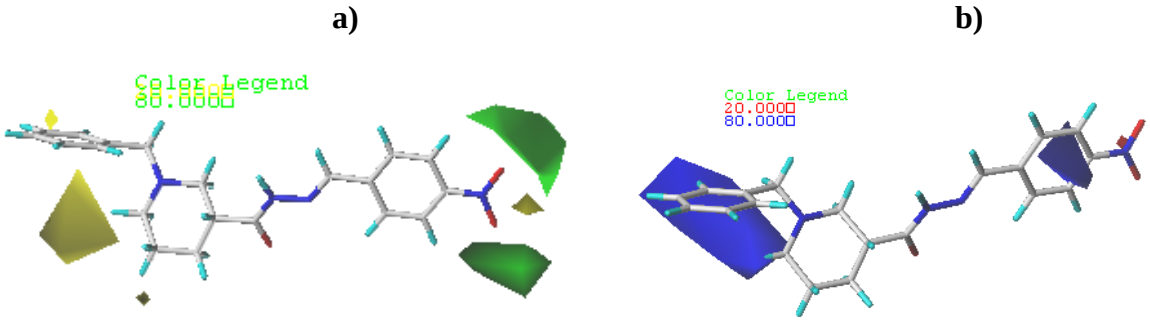

Figure 4: Contour maps of CoMSIA analysis. **a)** Steric fields; **b)** Electrostatic fields

3.1.2. CoMSIA Contour Map

The contour maps of CoMSIA steric field and electrostatic (Figures 5a and 5b) are almost identical to the corresponding CoMFA showing favored and disfavored regions. According to CoMSIA fractions presented in Table 2, H-bond acceptor and Hydrophobic fields (0.320 and 0.179) are the major fields that can describe the inhibitory activity.

In the hydrogen bond acceptors filed, as shown in Figure 5(c), the magenta (80% contribution) and red (20% contribution) contours represent favorable and unfavorable positions for H-bond acceptors respectively, to benefit the activity. A big-sized red contour is located close to the R1 and the C-2 positions of the phenyl moiety and another small one covers the N- of the piperidine illustrated unfavorable region where H-bond acceptor groups are not beneficial for the biological activity in these positions. In addition, another medium-sized magenta contour near the R1 position of the phenyl moiety indicates that a H-bond acceptor substituent at this position is predicted to benefit activity. For example, compound 7 {R_1= NO_2}, compound 17 {R_1 = NO_2}, compound 18 {R_1= CN} had the highest activities as indicated by pIC50 values of 5.246, 5.199, and 5.149, respectively, than that of compound 2 (pIC50 = 4.982), with CH_3 group at the same position.

In the hydrophobic field (Figure 5(e)), the yellow areas (80% contribution) represent areas where hydrophobic groups could increase biological activity, whereas white domains (20% contribution) designate areas where hydrophilic groups might increase the inhibitory activity. In our case there a very small white contour was observed on the bridge between the phenyl moiety and piperidine indicating that hydrophobic groups are not beneficial to the biological activity, while two large yellow contours are near the C-1 and C-2 positions of the piperidine and C-3 and C-4 of the left phenyl moiety linked to pyridine, indicating that a hydrophobic substituent at these positions might increase the inhibitory activity. The CoMSIA H-bond acceptor and hydrophobic interactions match well with the experimental results.

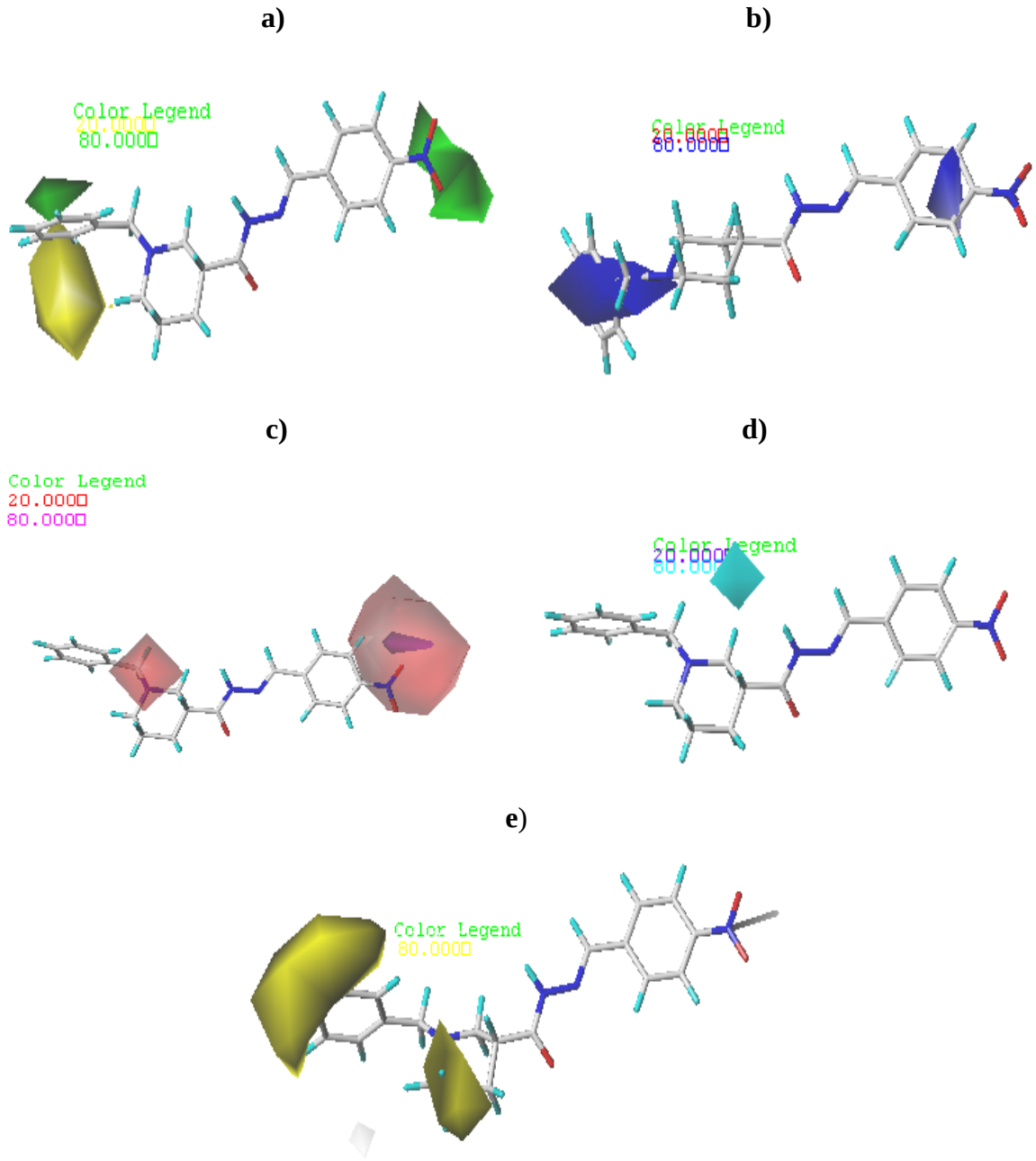

Figure 5: Contour maps of CoMSIA analysis. **a)** Steric field; **b)** Electrostatic field **c)** Hydrophobic field; **d)** H-bond acceptor field; **e)** H-bond donor field.

In figure 6, we summarized information from 3d contour maps results, which could be much helpful to design new molecules with high predictive activity.

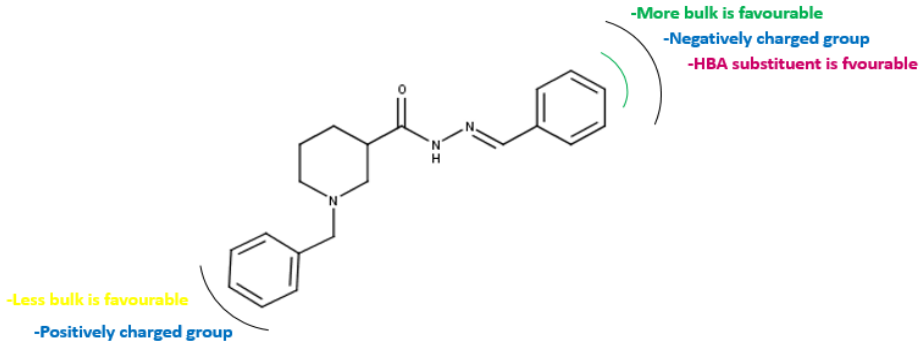

Figure 6: SAR summarized results

3.2.Y-Randomization

The 3D-QSAR is developed to further confirm the predictive potency of the CoMFA and CoMSIA, there were five shuffles of the dependent variable performed several times at random and after each iteration, a set of Q^2 and R^2 of new QSAR models is generated. As a result, (Table 4) the Q^2 and R^2 values were low which lead to conclude that the possibility of random correlations was ruled out.

Table 4: R^2 and Q^2 Values after Several Y-randomization Tests.

Iteration	CoMFA		CoMSIA	
	Q^2	R^2	Q^2	R^2
1	-0.122	-0.112	-0.242	0.326
2	0.254	0.395	0.267	0.292
3	-0.068	0.108	-0.179	-0.110
4	0.110	0.160	0.162	0.198
5	0.199	0.208	0.201	0.232
6	0.115	0.187	0.101	0.177
7	0.231	0.322	0.195	0.297

3.3.Design for new molecules with AChE inhibitors activity

According to the 3D-QSAR study, we designed five (A1-A5) new hydrazones derivatives by modifying chemical structure of the representative compound 7. The predicted activity of the proposed molecules showed effective inhibition of Alzheimer and higher binding affinities (total score) originating from various interactions contribution than that of compound 7 (pIC_{50}=5.240) for both models (Table 5 & Fig 7).

Table 5: New proposed molecules and their predicted pIC_{50}.

N°	Predicted pIC_{50}		Total Scoring
	CoMFA	CoMSIA	
Compound 7	5.246	5.245	3.986
A1	5.338	5.327	4.963
A1	5.306	5.302	4.688
A3	5.293	5.289	4.609
A4	5.249	5.248	4.321
A5	5.251	5.238	4.401

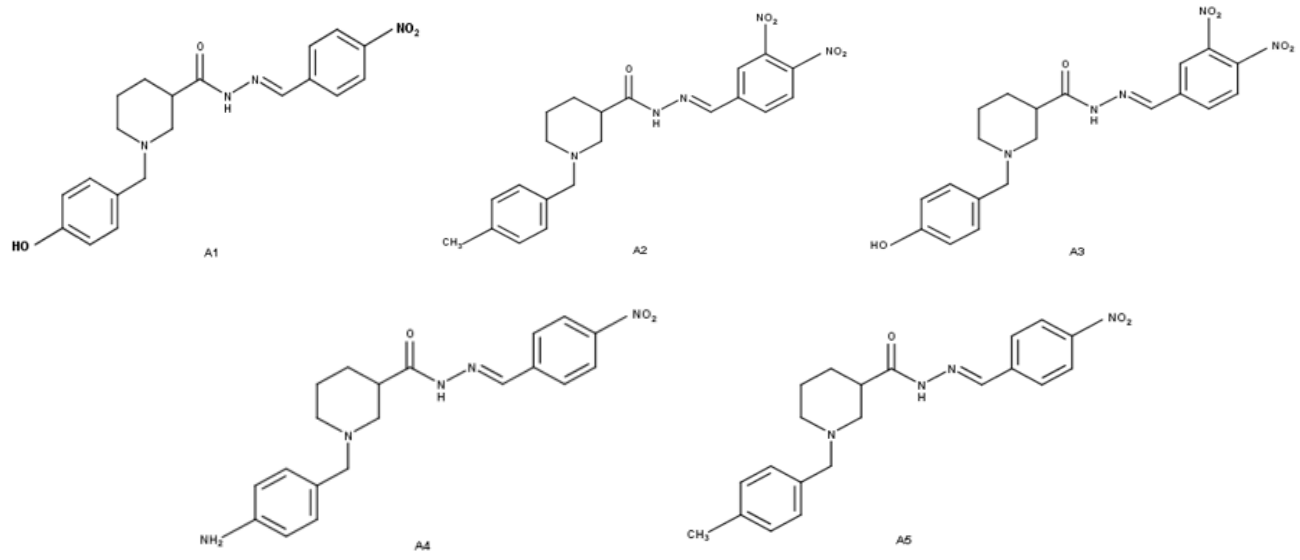

Figure 7: Structures of newly designed molecules.

3.4.Docking results

The molecular docking analysis was employed to investigate the different interactions of hydrazones derivatives inside the active site of the AChE receptor (code entry PDB: 1EVE). From the analysis in the figures 8 and 9, the highest active compound N° 7 and the proposed compound A1 were selected for detailed analysis, they are all well-superimposed in the ligand-binding pocket of the protein. The results of docking showed favorable and convenient interactions for compound 7 presenting a conventional hydrogen bond with Tyr 72 and Asp 72 residues generating from the piperidine and –NH- groups, respectively. Additional carbon hydrogen bond interaction of nitro group with active site residue His 440 was also observed, while the two phenyl moiety were in pi–pi stacked contact with Trp 279 and Phe 330 residues.

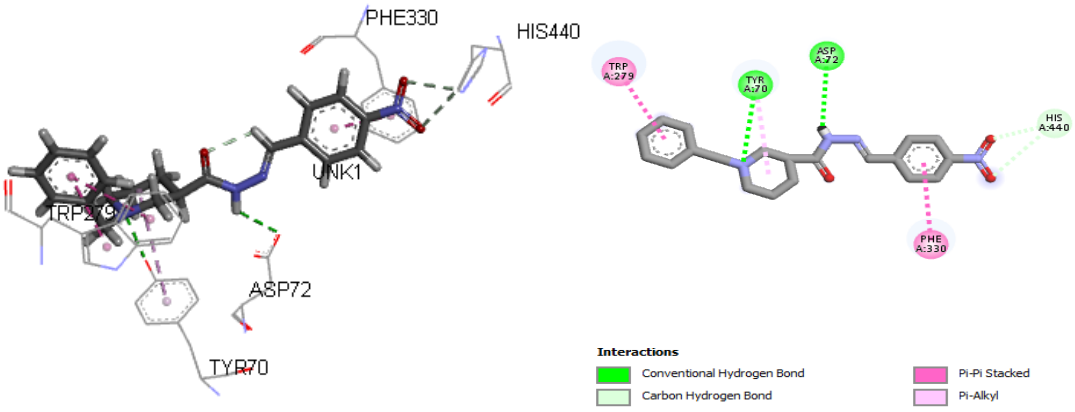

Figure 8: Docking interactions of the representative compound 7 with the receptor **1EVE**.

Figure 9 shows that the proposed compound A1 with hydrophobic character present conventional H-bond with Tyr 121, Asp 72, residues, H-bond interaction of oxygen atom generating from the phenyl moiety with active site residue Ser 200 was also observed. Furthermore, the docking results were compared with the QSAR results to confirm mutually the correlation, as a result, all new compounds entered the acetylcholinesterase binding pocket have the same or better docking pattern as the corresponding active compound 7. These binding interactions match well with the steric, electrostatic and H-bond acceptor contour maps analyses.

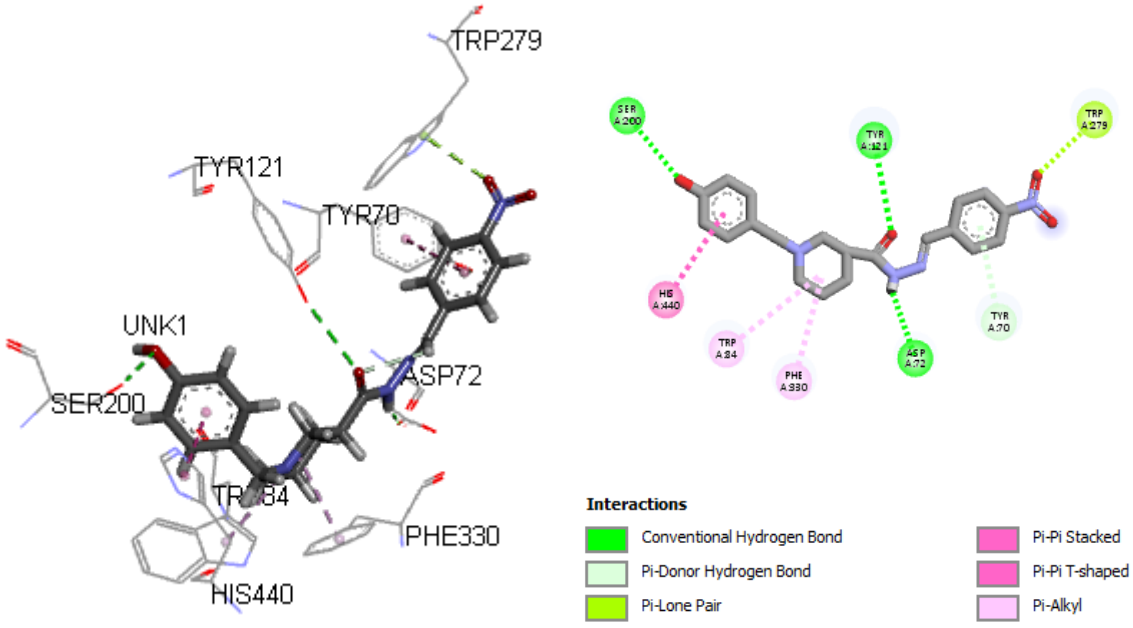

Figure 9: Docking interactions of the proposed compound with the receptor **1EVE**.

From the analysis, it was observed that the binding pattern of the proposed compound A1 with a total scoring 4.963 was better than that of the representative compound 7 with a total scoring 3.986 which supports the selected pose of the proposed compound. Thus, the overall obtained results not only provided in-depth understanding of the pattern interactions of these acetylcholinesterase inhibitors, but also demonstrates that hydrogen bonds have a key role in stabilizing the conformation of docking complex.

Conclusion

In the current study, a set of 20 hydrazones analogs identified as acetylcholinesterase inhibitors for Alzheimer disease was subjected to molecular modeling study. The application of the 3D-QSAR approach provided a valuable clue for the development of new potent hydrazones derivatives with higher affinities. In order to identify the various factors influencing the inhibitory activity, the obtained contour maps analyses clarified the effect and structural characteristics of several substituent in terms of favorable and unfavorable alternatives, as a result, five new Alzheimer's inhibitors were designed and showed improved inhibition activity. The docking analysis recognized important active site residues involved in the binding interactions of the proposed compound A1 and the most potent compound 7 with 1EVE receptor and indicated the reliability safety of the designed compounds.

Acknowledgements Great thanks to the "Association Marocaine des Chimistes Théoriciens" (AMCT) for its relevant help concerning the programs.

References

1. J. Wang, Z.M. Wang, X.M. Li, F. Li, J.J. Wu, L.Y. Kong, X.B. Wang, Synthesis and evaluation of multi-target-directed ligands for Alzheimer's disease based on the fusion of donepezil and melatonin, *Bioorg. Med. Chem.*, 24 (18) (2016) 4324-4338.
2. J.B. Shaik, B.K. Palaka, M. Penumala, K.V. Kotapati, S.R. Devineni, S. Eadlapalli, M.M. Darla, D.R. Ampasala, R. Vadde, G.D. Amooru, Synthesis, pharmacological assessment, molecular modeling and *in silico* studies of fused tricyclic coumarin derivatives as a new family of multifunctional anti-Alzheimer agents, *Eur. J. Med. Chem.* 107 (2016) 219-232.
3. P. Davies, J.F. Maloney, Selective loss of central cholinergic neurons in Alzheimer's disease, *Lancet.* 308 (1976) 1403.
4. A.I. Bush, The metal theory of Alzheimer's disease, *J. Alzheimers Dis.* 33 (Suppl1) (2013) 277–281.
5. A. Robert, Y. Liu, M. Nguyen, B. Meunier, Regulation of c and iron homeostasis by metal chelators: a possible chemotherapy for Alzheimer's disease, *Acc. Chem. Res*. 48 (2015) 1332–1339.
6. J. Hardy, D. Allsop, Amyloid deposition as the central event in the aetiology of Alzheimer's disease, *Trends Pharmacol. Sci.* 12 (1991) 383-388.
7. A. Tramutola, C. Lanzillotta, M. Perluigi, D.A. Butterfield, Oxidative stress, protein modification and Alzheimer disease, *Brain Res. Bull*. 133 (2017) 88-96.
8. M. P. Mattson, K. J. Tomaselli, R. E. Rydel, Calcium-destabilizing and neurodegenerative effects of aggregated beta-amyloid peptide are attenuated by basic FGF, *Brain Res.* 621 (1993) 35–49.
9. F. M. LaFerla, K. N. Green, S. Oddo, Intracellular amyloid-β in Alzheimer's disease, Nature *Rev. Neuro sci.* 8 (2007) 499–509.
10. R.D. Cramer III, D.E. Patterson, J.D. Bunnce. Comparative molecular field analysis (CoMFA): 1. Effect of shape on binding of steroids to carrier proteins. *J. Am. Chem. So.*, 110 (1988) 5959-5967.
11. G. Klebe, U. Abraham, T. Mietzner. Molecular similarity indices in a comparative analysis (CoMSIA) of drug molecules to correlate and predict their biological activity. *J. Med. Chem.*, 37 (1994) 4130-4146.
12. S. Parlar, G. Sayar, A. Hande Tarikogullari, S. Sozer Karadağli, V. Alptuzun, E. Erciyas, U. Holzgrabe, Synthesis, bioactivity and molecular modeling studies on potential anti-Alzheimer piperidinehydrazide-hydrazones, *Bioorganic Chemistry*. 87 (2018) 888-900, https://doi.org/10.1016/j.bioorg.2018.11.051
13. Tripos Inc., St. Louis, MO, USA, SYBYL-X 2.0, (n.d.). http://www.tripois.com.

14. M. Clark, R. D. Cramer, and N. Van Opdenbosch, 'Validation of the general purpose Tripos 5.2 force field', *Journal of Computational Chemistry,* 10 (8) (1989) 982–1012.
15. W.P. Purcell and J. A. Singer, A brief review and table of semiempirical parameters used in the Hueckel molecular orbital method, *Journal of Chemical and Engineemoiety Data,* 12 (2) (1967) 235–246.
16. M. D. M. AbdulHameed, A. Hamza, J. Liu, and C.-G. Zhan, Combined 3D-QSAR modeling and molecular docking study on indolinone derivatives as inhibitors of 3-phosphoinositide-dependent protein kinase-1, *Journal of chemical information and modeling.* 48 (9) (2008) 1760–1772.
17. L. Ståhle and S. Wold, 6 multivariate data analysis and experimental design in biomedical research, *in Progress in medicinal chemistry,* 25 (1988) 291–338.
18. B. L. Bush and R. B. Nachbar, Sample-distance partial least squares: PLS optimized for many variables, with application to CoMFA, *Journal of computer-aided molecular design*, 7 (5) (1993) 587–619.
19. A. Golbraikh, A. Tropsha, Beware of q2!, *J Mol Graph Model*, 20 (2002) 269–276, https ://doi.org/10.1016/S1093 -3263(01)00123 -1
20. A. Tropsha, P. Gramatica, V. K. Gombar, The importance of being earnest: validation is the absolute essential for successful application and interpretation of QSPR models. *QSAR Comb Sci* 22 (2003) 69–77, https ://doi.org/10.1002/qsar.20039 0007
21. M. Baroni , S. Clementi , G. Cruciani , G. Costantino , D. Riganelli , E. Oberrauch, Predictive ability of regression models. Part II: Selection of the best predictive PLS model. *J. Chemom*. 6(6) (1992) 347-56, https://doi.org/10.1002/cem.1180060605.
22. C. Rücker, G. Rücker, M. Memoiety er, y-Randomization and Its Variants in QSPR/QSAR, *J. Chem. Inf. Model.* 47 (2007) 2345-2357.
23. Sybyl 8.1; Tripos Inc.: St. Louis, MO, USA, 2008; Available online: http://www.tripos.com (accessed on 26 January 2011)
24. W. L. DeLano, The PyMOL molecular graphics system, Http://Pymol. Org. (2002).
25. Dassault Systèmes BIOVIA Discovery Studio Modeling Environment, Release 2017 Dassault Systèmes, (2016). http://accelrys.com/products/collaborative-science/biovia-discovery-studio/.

(2020) ; http://www.jmaterenvironsci.com